

AD-A056 946

DAYTON UNIV OHIO RESEARCH INST

F/G 20/4

A COMPARATIVE STUDY OF TWO COMPUTATIONAL METHODS FOR CALCULATING ETC(U)

NOV 77 D P RIZZETTA

F33615-76-C-3146

UNCLASSIFIED

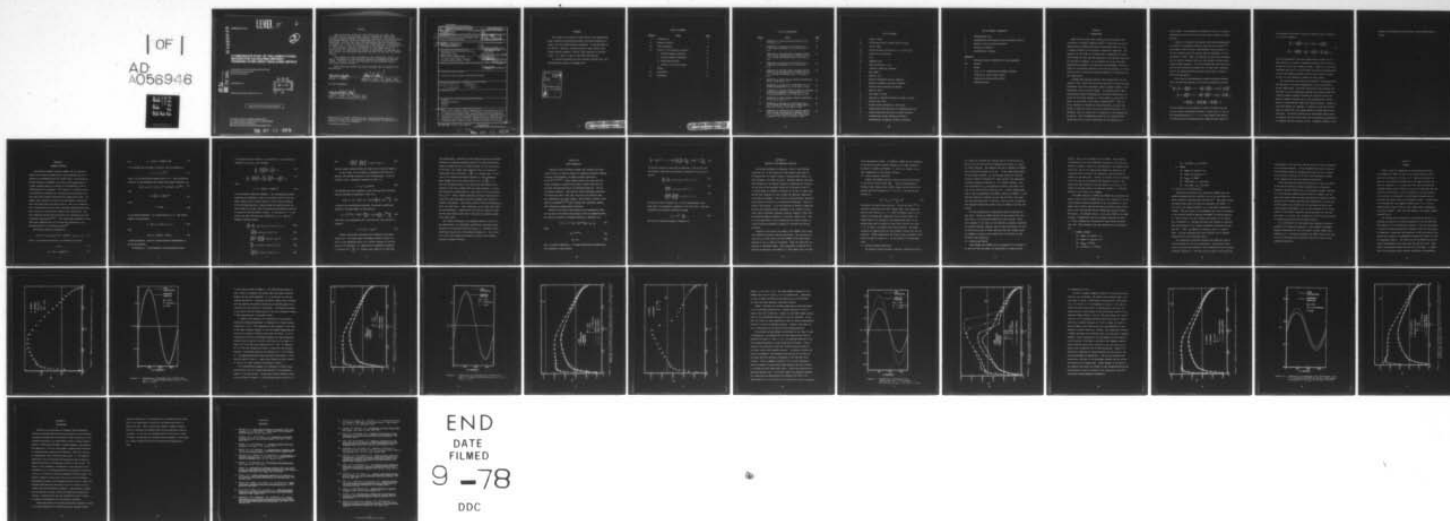
AFFDL-TR-77-118

NL

| OF |

AD
A066946

AD
A066946



AD A 056946

AFFDL-TR-77-118

LEVEL

II

2

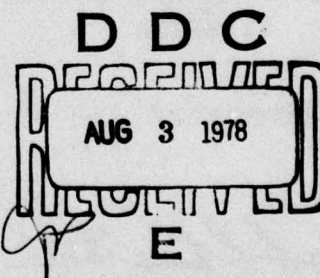
2

**A COMPARATIVE STUDY OF TWO COMPUTATIONAL
METHODS FOR CALCULATING UNSTEADY
TRANSONIC FLOWS ABOUT OSCILLATING AIRFOILS**

UNIVERSITY OF DAYTON RESEARCH INSTITUTE
300 COLLEGE PARK AVENUE
DAYTON, OHIO 45469

NOVEMBER 1977

TECHNICAL REPORT AFFDL-TR-77-118



Approved for public release; distribution unlimited.

AIR FORCE FLIGHT DYNAMICS LABORATORY
AIR FORCE WRIGHT AERONAUTICAL LABORATORIES
AIR FORCE SYSTEMS COMMAND
WRIGHT-PATTERSON AIR FORCE BASE, OHIO 45433

78 07 31 059

AD No.

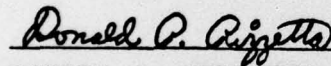
DDC FILE COPY

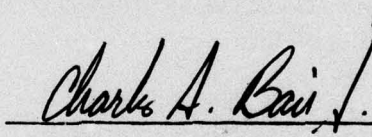
NOTICE

When Government drawings, specifications, or other data are used for any purpose other than in connection with a definitely related Government procurement operation, the United States Government thereby incurs no responsibility nor any obligation whatsoever; and the fact that the Government may have formulated, furnished, or in any way supplied the said drawings, specifications, or other data, is not to be regarded by implication or otherwise as in any manner licensing the holder or any other person or corporation, or conveying any rights or permission to manufacture, use, or sell any patented invention that may in any way be related thereto.

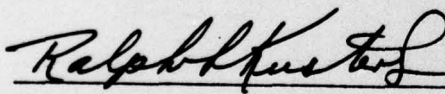
This report has been reviewed by the Information Office (OI) and is releasable to the National Technical Information Service (NTIS). At NTIS, it will be available to the general public, including foreign nations.

This technical report has been reviewed and is approved for publication.


DONALD P. RIZZETTA


CHARLES A. BAIR, JR., MAJOR, USAF
Chief, Analysis & Optimization Branch

FOR THE COMMANDER


RALPH L. KUSTER, JR., COLONEL, USAF
Chief, Structural Mechanics Division

Copies of this report should not be returned unless return is required by security considerations, contractual obligations, or notice on a specific document.

UNCLASSIFIED

SECURITY CLASSIFICATION OF THIS PAGE (When Data Entered)

REPORT DOCUMENTATION PAGE		READ INSTRUCTIONS BEFORE COMPLETING FORM
1. REPORT NUMBER AFFDL TR-77-118	2. GOVT ACCESSION NO.	3. RECIPIENT'S CATALOG NUMBER
4. TITLE (and Subtitle) A Comparative Study of Two Computational Methods for Calculating Unsteady Transonic Flows About Oscillating Airfoils	5. TYPE OF REPORT & PERIOD COVERED FINAL REPORT April - June 1977	
6. AUTHOR(s) Dr. Donald P. Rizzetta (Visiting Scientist)	7. PERFORMING ORG. REPORT NUMBER	
8. CONTRACT OR GRANT NUMBER(s) F33615-76-C-3146 new	9. PROGRAM ELEMENT, PROJECT, TASK AREA & WORK UNIT NUMBERS P.E. 61102F Project 2307 Task 230705/Work Unit 23070501	
10. CONTROLLING OFFICE NAME AND ADDRESS Air Force Flight Dynamics Laboratory Wright-Patterson AFB, Ohio 45433	11. REPORT DATE November 1977	
12. MONITORING AGENCY NAME & ADDRESS (if different from Controlling Office)	13. NUMBER OF PAGES 12/43p.	
14. DISTRIBUTION STATEMENT (of this Report) Approved for Public Release; Distribution Unlimited	15. SECURITY CLASS. (of this report) UNCLASSIFIED 15a. DECLASSIFICATION/DOWNGRADING SCHEDULE	
16. DISTRIBUTION STATEMENT (of the abstract entered in Block 20, if different from Report) 2307 05		
17. SUPPLEMENTARY NOTES		
18. KEY WORDS (Continue on reverse side if necessary and identify by block number) Transonic Unsteady Aerodynamics Airfoils Flutter		
19. ABSTRACT (Continue on reverse side if necessary and identify by block number) This report provides a direct comparison of the calculations for the flow field about an oscillating airfoil in a transonic freestream predicted by two computational methods; namely, harmonic analysis and time integration. Details of the two methods are summarized and results for NACA64A010 airfoil oscillating in pitch are considered. Comparisons of the unsteady pressure distribution and resultant lift are presented for several values of free-stream Mach number, angle of attack, and reduced frequency of oscillation.		

DD FORM 1 JAN 73 1473

EDITION OF 1 NOV 65 IS OBSOLETE

UNCLASSIFIED

SECURITY CLASSIFICATION OF THIS PAGE (When Data Entered)

105 400

78 07 31 059

act

FOREWORD

This report is the result of work carried in the Optimization Group, Analysis and Optimization Branch, Structural Mechanics Division, Air Force Flight Dynamics Laboratory. It was performed by Dr. Donald P. Rizzetta, visiting scientist, under Project 2307, "Flight Vehicle Dynamics," Task 05, "Basic Research in Aeroelasticity." Dr. James J. Olsen is the AFFDL Task Engineer.

Dr. Rizzetta performed the work from April through June, 1977 and released the report in September 1977.

ACCESSION for		
NTIS	White Section	<input checked="" type="checkbox"/>
DDC	Buff Section	<input type="checkbox"/>
UNANNOUNCED		<input type="checkbox"/>
JUSTIFICATION.....		
BY.....		
DISTRIBUTION/AVAILABILITY CODES		
Dist.	AVAIL. and/or SPECIAL	
A		

TABLE OF CONTENTS

<u>Section</u>	<u>Title</u>	<u>Page</u>
I	Introduction	1
II	Harmonic Analysis	5
III	Time Integration	10
IV	Details of the Numerical Solutions	12
	1. Airfoil Boundary Conditions	13
	2. Farfield Boundary Conditions	13
	3. Computational Meshes	14
	4. Accuracy of the Calculations	16
V	Results	18
VI	Conclusions	33
VII	References	35

LIST OF ILLUSTRATIONS

<u>Figure</u>	<u>Title</u>	<u>Page</u>
1	Comparison of Steady Surface Pressure for $M_\infty = 0.72$ and $\alpha = 0$	19
2	Comparison of Unsteady Lift Coefficient for a 1° Pitching Oscillation at $M_\infty = 0.72$ and $k = 0.05$	20
3	Comparison of Unsteady Surface Pressure Coefficient at Time Corresponding to Maximum Lift for a 1° Pitching Oscillation at $M_\infty = 0.72$ and $k = 0.05$	22
4	Comparison of Unsteady Lift Coefficient for a 1° Pitching Oscillation at $M_\infty = 0.72$ and $k = 0.20$	23
5	Comparison of Unsteady Surface Pressure Coefficient at Time Corresponding to Maximum Lift for a 1° Pitching Oscillation at $M_\infty = 0.72$ and $k = 0.20$	24
6	Comparison of Steady Surface Pressure Coefficient for $M_\infty = 0.82$ and $\alpha = 0^\circ$	25
7	Comparison of Unsteady Lift Coefficient for a 1° Pitching Oscillation at $M_\infty = 0.82$ and $k = 0.05$	27
8	Comparison of Unsteady Surface Pressure Coefficient at Time Corresponding to Maximum Lift for a 1° Pitching Oscillation at $M_\infty = 0.82$ and $k = 0.05$	28
9	Comparison of Steady Surface Pressure Coefficient for $M_\infty = 0.72$ and $\alpha = 1^\circ$	30
10	Comparison of Unsteady Lift Coefficient for a 0.5° Pitching Oscillation about a Mean Angle of Attack of 1° at $M_\infty = 0.72$ and $k = 0.05$	31
11	Comparison of Unsteady Surface Pressure Coefficient at Time Corresponding to Maximum Lift for a 0.5° Pitching Oscillation about a Mean Angle of Attack of 1° at $M_\infty = 0.72$ and $K = 0.05$	32

LIST OF SYMBOLS

a	speed of sound
b_n	coefficients used to define airfoil surface
c	airfoil chord
C_p	section pressure coefficient, $(p - p_\infty)/1/2 \rho_\infty U_\infty^2$
C_ℓ	section lift coefficient
i	$\sqrt{-1}$
Im	imaginary part
k	reduced frequency, $\omega c/U_\infty$
K	transonic similarity parameter
M	Mach number
t	physical time
u	physical streamwise velocity component
x	physical streamwise Cartesian coordinate
y	physical normal Cartesian coordinate
α	angle of attack
α_s	mean angle of attack
α_u	amplitude of unsteady variation in angle of attack
γ	specific heat ratio
δ	maximum airfoil thickness to chord ratio
$\Delta\xi$	computational mesh step size in streamwise direction
$\Delta\eta$	computational mesh step size in normal direction
η	nondimensional normal Cartesian coordinate
ξ	nondimensional streamwise Cartesian coordinate

LIST OF SYMBOLS (CONTINUED)

τ	nondimensional time
ϕ	nondimensional perturbation velocity potential function
Φ	physical velocity potential function
ω	oscillation frequency
Ω	nondimensional frequency

Subscript

B	Ballhaus-Goorjian formulation for time integration
min	minimum
s	steady
T	Traci, et al. formulation for harmonic analysis
+	evaluated on airfoil upper surface
-	evaluated on airfoil lower surface
∞	freestream value

SECTION I

INTRODUCTION

While there has been great progress in recent years in the calculation of unsteady transonic flows⁽¹⁾, rarely have any of the computational procedures which have evolved been applied to a set of similar problems for the purpose of analytical comparison. The objective of this study is to provide such a comparison for two of these methods in order that the character of the resultant solutions for each may be examined. As the ultimate use of any flow field computational procedure is to establish the aerodynamic forces necessary for performance evaluation and structural analysis, it is the intention here to indicate the expected behavior of calculations for such applications.

Although many unsteady transonic flow problems have been considered to date, there exist only three approaches by which unsteady aerodynamic forces may be obtained; namely, harmonic analysis, time integration, and the indicial method. The indicial method, while having certain inherent advantages for structural applications, requires the flow field response to a step change in a given mode of motion of the airfoil or body under consideration⁽²⁾. This "indicial response" is obtained via time integration, and thus this method, in spirit at least, will not be considered distinct. We, therefore, limit our attention to a comparison of the remaining two procedures. Only two-dimensional flows will be considered here, though this is not a strict requirement for the application of

either method. This assumption considerably reduces the necessary computations without loss of any of the salient features of either approach.

A number of successful calculations have been performed which are capable of describing transonic flows over blunt bodies⁽³⁻⁷⁾. These employ either the exact time-dependent Euler equations, or the full unsteady potential equation when the assumption of irrotationality is made. While such methods are often time consuming, they are able to properly treat the time behavior of bodies oscillating at high frequency. It will be assumed here that the body is thin and the oscillation frequency low, in which case a limiting form of the complete potential equation may be used to obtain a flow field description.

In the case of two-dimensional inviscid irrotational unsteady flow, the governing equation for the velocity potential function is:

$$\begin{aligned} \frac{\partial^2 \Phi}{\partial t^2} + \left\{ (\gamma + 1) \left(\frac{\partial \Phi}{\partial x} \right)^2 / 2 + (\gamma - 1) \left[\frac{\partial \Phi}{\partial t} + \left(\frac{\partial \Phi}{\partial y} \right)^2 / 2 - U_\infty^2 / 2 \right] - a_\infty^2 \right\} \frac{\partial^2 \Phi}{\partial x^2} \\ + \left\{ (\gamma + 1) \left(\frac{\partial \Phi}{\partial y} \right)^2 / 2 + (\gamma - 1) \left[\frac{\partial \Phi}{\partial t} + \left(\frac{\partial \Phi}{\partial x} \right)^2 / 2 - U_\infty^2 / 2 \right] - a_\infty^2 \right\} \frac{\partial^2 \Phi}{\partial y^2} \quad (1) \\ + 2 \frac{\partial \Phi}{\partial x} \frac{\partial^2 \Phi}{\partial x \partial t} + 2 \frac{\partial \Phi}{\partial x} \frac{\partial \Phi}{\partial y} \frac{\partial^2 \Phi}{\partial x \partial y} + 2 \frac{\partial \Phi}{\partial y} \frac{\partial^2 \Phi}{\partial y \partial t} = 0. \end{aligned}$$

If this equation is to be applied in order to describe the flow over an airfoil with maximum thickness to chord ratio, δ , then in the limiting process $M_\infty \rightarrow 1$, $\delta \rightarrow 0$, a much simpler form results. A careful study of the characteristic length and time scales for

low frequency oscillations reveals the dominant terms of Equation 1 to be the following:

$$\left\{ (\gamma + 1) \left(\frac{\partial \Phi}{\partial x} \right)^2 / 2 - [(\gamma - 1) U_\infty^2 / 2 + a_\infty^2] \right\} \frac{\partial^2 \Phi}{\partial x^2} \quad (2)$$

$$+ \left\{ (\gamma - 1) \left[\left(\frac{\partial \Phi}{\partial x} \right)^2 - U_\infty^2 \right] / 2 - a_\infty^2 \left\{ \frac{\partial^2 \Phi}{\partial y^2} + 2 \frac{\partial \Phi}{\partial x} \frac{\partial^2 \Phi}{\partial x \partial t} \right\} \right\} = 0.$$

In actual application, even more simplification follows as it is only necessary to include the dominant nonlinear term in order to account for first order transonic effects. Equation 2 is the form considered here and it is noted because the specific implementation of one of the methods analyzed leaves the time variable unscaled so that it is not possible to deduce its exact origin.

For this study, one airfoil was selected for investigation and was prescribed to oscillate sinusoidally in time in one mode of motion, namely pitch. Flow field calculations were performed and solutions to the two-dimensional unsteady low frequency small disturbance transonic potential equation was obtained by both the method of harmonic analysis and by time integration for several values of freestream Mach number and reduced frequency. Results of these calculations are compared. It should be noted that neither method is restricted to the single degree of freedom (pitch) selected here. The airfoil chosen was an NACA 64A010 airfoil which is symmetric and ten percent thick, and is considered representative of transonic airfoils currently in use. Asymmetric behavior is ex-

amed by oscillating the airfoil about a mean nonzero angle of attack.

SECTION II

HARMONIC ANALYSIS

The method of harmonic analysis assumes that the unsteady motion of an airfoil oscillating with small amplitude may be regarded as a perturbation about the steady state. The velocity potential function is expanded in a series of increasing powers of a small parameter which is a measure of the amplitude of the unsteady motion of the boundary. This results in a sequence of partial differential equations for the perturbation potentials with the zeroth order equation recovering the steady-state result. All higher order equations are linear with non-constant coefficients which now depend upon the steady solution. This set of equations may be solved using the well known relaxation algorithms which have been utilized for steady-state transonic flow calculations. Harmonic analysis has been used successfully for unsteady airfoil and rectangular wing motions⁽⁸⁻¹²⁾. The leading order equations of this method are summarized here for the specific application to the pitching motion of an oscillating airfoil⁽⁹⁾.

The velocity potential is written as

$$\Phi(x, y, t) = U_{\infty}x + U_{\infty}c\delta^{2/3}[(1 + \gamma)M_{\infty}^2]^{-1/3} \phi_T(\xi, \eta_T, \tau_T) \quad (3)$$

where c is the airfoil chord and δ the thickness ratio with

$$\xi = x/c, \quad (4)$$

$$\eta_T = y[(1 + \gamma)\delta M_{\infty}^2]^{1/3}/c, \quad (5)$$

and
$$\tau_T = U_\infty t [(1 + \gamma) \delta M_\infty^2]^{2/3} / c M_\infty^2. \quad (6)$$

It is assumed that the angle of attack α , may be expressed as

$$\alpha = \alpha_s + \alpha_u e^{i\omega t} \quad (7)$$

where ω is the oscillation frequency and $\alpha/\delta \ll 1$. The perturbation potential is now decomposed into steady and unsteady components, as

$$\phi_T(\xi, \eta_T, \tau_T) = \phi_s(\xi, \eta_T) + (\alpha_u/\delta) \phi_u(\xi, \eta_T) e^{i\Omega \tau_T}. \quad (8)$$

Here

$$\Omega = k M_\infty^2 [(1 + \gamma) \delta M_\infty^2]^{-2/3} \quad (9)$$

where

$$k = \omega c / U_\infty \quad (10)$$

is the reduced frequency. It is noted that $\Omega \tau_T = \omega t$. The airfoil boundary is described by

$$y - F(x, t) = 0 \text{ for } 0 \leq x \leq c \quad (11)$$

with

$$F(x, t) = c\delta [f(\xi) - \alpha\xi/\delta], \quad (12)$$

α given by Equation 7 and $f(\xi)$ a known function corresponding to the airfoil geometry.

If Equations 3 - 6 and Equation 8 are now substituted into

the reduced potential Equation 2 (or Equation 1), the following expressions for ϕ_s and ϕ_u are obtained:

$$\left(K - \frac{\partial \phi_s}{\partial \xi} \right) \frac{\partial^2 \phi_s}{\partial \xi^2} + \frac{\partial^2 \phi_s}{\partial \eta_T^2} = 0, \quad (13)$$

$$\left(K - \frac{\partial \phi_s}{\partial \xi} \right) \frac{\partial^2 \phi_u}{\partial \xi^2} + \frac{\partial^2 \phi_u}{\partial \eta_T^2} - \left(\frac{\partial^2 \phi_s}{\partial \xi^2} + 2i\Omega \right) \frac{\partial \phi_u}{\partial \xi} = 0, \quad (14)$$

where

$$K = (1 - M_\infty^2) [(1 + \gamma) \delta M_\infty^2]^{-2/3} \quad (15)$$

is the transonic similarity parameter. The corresponding boundary conditions for Equations 13 and 14 are obtained from the flow tangency condition on the airfoil surface, from the Kutta condition at the trailing edge with a constant jump in potential across the vortex sheet in the wake, and by requiring the perturbation velocity to vanish far from the airfoil surface. In the limit as $\delta \rightarrow 0$, the airfoil and wake conditions may be applied on $y = 0$. Thus the boundary conditions become

$$\frac{\partial \phi_s}{\partial \eta_T} = \frac{df}{d\xi} - \alpha_s / \delta \text{ on } \eta_T = 0 \text{ for } 0 \leq \xi \leq 1, \quad (16)$$

$$\left[\frac{\partial \phi_s}{\partial \xi} \right] = 0 \text{ on } \eta_T = 0 \text{ for } \xi > 1, \quad (17)$$

$$\left(\frac{\partial \phi_s}{\partial \xi} \right)^2 + \left(\frac{\partial \phi_s}{\partial \eta_T} \right)^2 \rightarrow 0 \text{ as } \xi^2 + \eta_T^2 \rightarrow \infty, \quad (18)$$

$$\frac{\partial \phi_u}{\partial \eta_T} = -1 \text{ on } \eta_T = 0 \text{ for } 0 \leq \xi \leq 1, \quad (19)$$

$$\left[\frac{\partial \phi_u}{\partial \xi} \right] = 0 \text{ on } \eta_T = 0 \text{ for } \xi > 1, \quad (20)$$

and
$$\left(\frac{\partial \phi_u}{\partial \xi}\right)^2 + \left(\frac{\partial \phi_u}{\partial \eta_T}\right)^2 \rightarrow 0 \text{ as } \xi^2 + \eta_T^2 \rightarrow \infty. \quad (21)$$

Here the square brackets denote the "jump" in the enclosed quantity.

In this study, for the purpose of comparison with time integration, the unsteady variation of the pitching angle, α , was prescribed to have a sinusoidal variation in time; i.e.,

$$\alpha = \alpha_s + \alpha_u \sin(\omega t). \quad (22)$$

The unsteady flow field response to this variation may be obtained from the solutions to Equations 13 and 14 as

$$\phi_T(\xi, \eta_T, \tau_T) = \phi_s(\xi, \eta_T) + (\alpha_u/\delta) \text{Im} \left[\phi_u(\xi, \eta_T) e^{i\Omega \tau_T} \right]. \quad (23)$$

In terms of the perturbation potential, the pressure coefficient defined in the usual manner is then given by

$$C_p = -2\delta^{2/3} [(1 + \gamma) M_\infty^2]^{-1/3} \left[\frac{\partial \phi_s}{\partial \xi} + (\alpha_u/\delta) \text{Im} \left(\frac{\partial \phi_u}{\partial \xi} e^{i\Omega \tau_T} \right) \right], \quad (24)$$

from which the corresponding lift coefficient per unit span may be obtained:

$$C_l = \int_0^1 (C_{p-} - C_{p+}) d\xi. \quad (25)$$

Several observations concerning this formulation seem appropriate here. The steady small disturbance transonic equation exhibits a type dependence which is in itself a function of the solution of the equation; i.e., Equation 13 is hyperbolic, parabolic, or elliptic for $\left(\frac{\partial \phi_s}{\partial \xi} - K \right)$ greater than, equal to, or less than

zero respectively. Solutions to this equation have been efficiently obtained by relaxation procedures based on the mixed differencing scheme of Murman and Cole (13) which accounts for the local nature of the flow. For a given flow situation, then, the location of "shock waves" will occur where $(\frac{\partial \phi_s}{\partial \xi} - K)$ changes sign. In the case of the unsteady perturbation Equation 14, type dependence again depends only on the steady result (i.e., on $\frac{\partial \phi_s}{\partial \xi} - K$). Thus the unsteady position of any shock waves which form is constrained to vary only slightly from the steady location. In fact, this variation is proportional to (α_u/δ) where it will be recalled that $\alpha_u/\delta \ll 1$. Hence, harmonic analysis precludes a description of large scale shock excursions which have commonly been observed in transonic experiments. This results directly from the linearization about the steady state. Time integration, on the other hand, makes no such assumptions. Comparison of the results of these two methods will help indicate under which conditions the harmonic assumptions remain valid.

One distinct advantage of the harmonic method is that due to the linearization, all aerodynamic coefficients now become linear functions of the unsteady deflection angle, α_u . Therefore, these coefficients depend only on the reduced frequency, k . Such is not true of the time integration technique, because of the complete nonlinear treatment involved.

SECTION III

TIME INTEGRATION

Numerical finite difference schemes that integrate the equations of motion in time are capable of simulating nonlinear unsteady transonic flow phenomena, including irregular shock wave motions^(1,3-6,14-17). These schemes usually rely upon shock capturing techniques to resolve shock waves, thereby requiring conservative differencing form of the governing equations. This is not always convenient. Time explicit finite difference procedures (3-6) generally have a time step restriction for stability such that computations are often lengthy. More recently, however, fully implicit techniques⁽¹⁷⁻¹⁹⁾ have relieved this constraint, making time integration computationally efficient.

Details of the form of the equation to be integrated in time for the case of an airfoil oscillating in pitch are summarized here. The velocity potential is expanded similarly to Equation 3 as

$$\phi(x, y, t) = U_{\infty}x + U_{\infty}c\delta^{2/3}\phi_B(\xi, \eta_B, \tau_B) \quad (26)$$

where

$$\eta_B = y\delta^{1/3}/c, \quad (27)$$

$$\tau_B = \omega t, \quad (28)$$

and ξ is given by Equation 4. If these definitions are substituted into Equation 2, there results

$$\left[(1 - M_\infty^2) \delta^{-2/3} - (1 + \gamma) M_\infty^2 \frac{\partial \phi_B}{\partial \xi} \right] \frac{\partial^2 \phi_B}{\partial \xi^2} + \frac{\partial \phi_B}{\partial \eta_B^2} = 2k M_\infty^2 \delta^{-2/3} \frac{\partial^2 \phi_B}{\partial \xi \partial \tau_B}. \quad (29)$$

The airfoil surface is described by Equations 11 and 12 such that the boundary conditions corresponding to Equation 29 are the following:

$$\frac{\partial \phi_B}{\partial \eta_B} = \frac{df}{d\xi} - \alpha/\delta \text{ on } \eta_B = 0 \text{ for } 0 \leq \xi \leq 1, \quad (30)$$

$$\left[\frac{\partial \phi_B}{\partial \xi} \right] = 0 \text{ on } \eta_B = 0 \text{ for } \xi > 1, \quad (31)$$

$$\left(\frac{\partial \phi_B}{\partial \xi} \right)^2 + \left(\frac{\partial \phi_B}{\partial \eta_B} \right)^2 \rightarrow 0 \text{ as } \xi^2 + \eta^2 \rightarrow \infty. \quad (32)$$

We note here that in Equation 30, α is the instantaneous pitch angle which is prescribed by Equation 22 for this study. With this formulation the pressure coefficient becomes

$$C_p = -2\delta^{2/3} \frac{\partial \phi_B}{\partial \xi}, \quad (33)$$

and the lift follows according to Equation 25.

SECTION IV

DETAILS OF THE NUMERICAL SOLUTIONS

We now seek solutions to Equations 13 and 14 with boundary conditions 16 - 21 and Equation 29 with boundary conditions 30 - 32 respectively for several values of freestream Mach number, reduced frequency, and angle of attack. Existing computer codes have been developed for the express purpose of obtaining such solutions for the form of the equations arrived at in Sections II and III. A certain amount of freedom is available to the user of these codes and has been exercised in order to make the resultant comparisons as reliable as possible. Each code has certain prominent characteristics which are central to its respective formulation. These are noted in this section. It is the intention to achieve a comparison between the alternative basic treatments of the unsteady low frequency small disturbance transonic potential equation, rather than any numerical behavior inherent to a specific computer code. This is not an easy task as we are dealing with the actual solution of finite difference equations as opposed to nonlinear differential equations.

Equation 13 was solved via computer code STRANS2 (9,20) using the relaxation procedure mentioned previously. The resulting solution for ϕ_s is then input into code UTRANS2 (9,20) which solves Equation 14 for ϕ_u , again by relaxation. These two codes were formulated for compatible usage. Time integration of Equation 29 is achieved by employing code LTRAN2 (17), which makes use of an effi-

cient time-implicit method. In addition, LTRAN2 has the capability of solving the steady transonic equation by the same relaxation procedure of STRANS2 and UTRANS2. It will be of interest to consider comparisons of some steady solutions.

4.1 Airfoil Boundary Conditions

STRANS2 and UTRANS2 require as input an analytic description of the airfoil surface slope, $\frac{df}{d\xi}$. This was accomplished by fitting a least squares curve to NACA tabular airfoil data for an assumed functional dependence of f on ξ (21). The function was selected as

$$f(\xi) = b_{1/2} \xi^{1/2} + \sum_{n=0}^5 b_n \xi^n \quad (34)$$

from which the slope follows directly. We note the term $\xi^{1/2}$ is included to approximate the blunt leading edge, thus, making the surface slope infinite at $\xi = 0$. Small disturbance theory is incapable of treating this singularity and in general either the leading edge is not included in the computational mesh, or the leading edge slope is modified to some finite value in the limit $\xi \rightarrow 0$, in order to accomodate blunt nosed airfoils. The former technique was employed here for both harmonic analysis and time integration. LTRAN2 approximates the airfoil slope by passing a cubic spline through the tabular data and extracting the corresponding slope.

4.2 Farfield Boundary Conditions

The harmonic farfield boundary condition, Equations 18 and 21,

are treated by obtaining the limiting form of the potentials (ϕ_s and ϕ_u) far from the airfoil and applying this result at a large but finite distance. This approach was used in STRANS2 and UTRANS2 with considerable savings in the extent of the computational mesh. For the steady potential, ϕ_s , the limiting form is the farfield condition derived by Klunker (22), which results from application of Green's theorem to Equation 13. In a similar fashion, a farfield expression for ϕ_u was obtained in terms of the Hankel function of the second kind of order zero (9). A finite series expansion is used to approximate this Hankel function in UTRANS2. If the farfield condition is applied too far from the body it was found that this series may fail to converge. This fact was of importance when numerical meshes were chosen as will be shown in the next subsection.

For time integration, no approximate farfield condition has been found. Therefore, LTRAN2 applies the mean steady-state limiting form of the potential extremely far from the body. While this treatment is not exact, it has produced no numerical anomalies. The farfield boundary, however, must be taken sufficiently far from the airfoil such that no waves reflected from this boundary reach the immediate vicinity of the airfoil over the interval of time covered by the integration.

4.3 Computational Meshes

Codes STRANS2 and UTRANS2 have the capability of accepting input data for both the number and distribution of numerical mesh

points. This is not in general true of LTRAN2. As the spatial differencing of the finite difference equations of the time integration in LTRAN2 is similar to that employed by the harmonic analysis codes, then if the computational meshes are identical, the truncation error incurred in the respective solutions should be formally of the same order. Because the scaling of the y-coordinate is not the same for both methods (see Equations 5 and 27), the meshes were made identical by forcing values of η_T and η_B to correspond to the same value of the physical variable, y. Identical values of ξ were used in all programs.

The meshes employed in STRANS2 and UTRANS2 were truncated versions of the one used in LTRAN2 because of the treatment of the far-field boundary conditions described in the last subsection. Both meshes used 33 points distributed along the airfoil surface with a point at the trailing edge and the leading edge situated between mesh points. The minimum ξ -step, $\Delta \xi_{\min}$, was 0.00330 at the leading edge. Minimum mesh sizes in the normal direction occurred at $y = 0$ with a symmetrical distribution of points above and below this axis. Mesh boundaries and other pertinent data are given below:

a. STRANS2, UTRANS2

- (1) number of ξ -points = 70
- (2) number of η_T -points = 43
- (3) $\Delta \eta_{T\min} = 0.02151$
- (4) $-8.19140 \leq \xi \leq 9.02411$

$$(5) \quad -10.13300 \leq \eta_T \leq 10.13300$$

b. LTRAN2

$$(1) \quad \text{number of } \xi\text{-points} = 99$$

$$(2) \quad \text{number of } \eta_B\text{-points} = 79$$

$$(3) \quad \Delta\eta_{Bmin} = 0.02000$$

$$(4) \quad -1033.53047 \leq \xi \leq 855.91313$$

$$(5) \quad -811.12200 \leq \eta_B \leq 811.12200$$

4.4 Accuracy of the Calculations

Steady-state solutions for ϕ_s provided by STRANS2 were considered converged when the variation in ϕ_s at all mesh points between consecutive iterations was less than 10^{-5} . This same criteria was applied when steady solutions were obtained from LTRAN2. In the case of the complex potential, ϕ_u , a less severe standard was invoked. This was because of the extremely slow rate of convergence of the solution procedure employed by UTRANS2 for solving Equation 14. More accuracy in ϕ_s was insisted upon because of its appearance in Equation 14. Unsteady solutions were accepted as converged when the variation in $|\phi_u|$ between consecutive iterations was less than 10^{-4} . Here, $|\phi_u|$ implies the absolute value in a complex sense. This was considered more than sufficient for an adequate comparison with time integrated results.

The steady-state solutions obtained from LTRAN2 were used as initial profiles for all time integrations. Starting with these values, solutions were advanced in time invoking the forced boundary condition, Equation 22. The time step size used for any given case

corresponded to 360 time steps over one period of forced oscillation at the reduced frequency. It was determined that such a time step was sufficiently small by increasing this value by up to a factor of five without variation in the first three significant figures of the computed lift and local pressure coefficients.

After solutions were advanced sufficiently in time, the effect of the initial conditions became negligible and the solutions attained a periodic behavior due to the periodic boundary condition. It is this periodic behavior which we desire to compare, not the small time history which can never be predicted by harmonic analysis. Solutions were considered periodic when repeatability to three significant figures was attained over two successive periods by all local pressure coefficients. For the cases examined in this study, effects of the initial conditions usually persisted for less than one period. As a result all solutions were forced for three periods of oscillation starting from the initial profile.

Lift coefficients for both methods were computed according to Equation 25 by numerical integration. Codes STRANS2 and UTRANS2 employed trapezoidal rule for this purpose, whereas LTRAN2 used a Simpson's rule. Although this renders the LTRAN2 results more accurate, both techniques were considered sufficiently exact for the comparisons made here.

SECTION V

RESULTS

Figure 1 shows the comparison of the steady-state results from STRANS2 and LTRAN2 in terms of the surface pressure coefficient for the case $M_\infty = 0.72$ and $\alpha = 0$. Because the airfoil is symmetric, the pressure distributions on the upper and lower surfaces are identical. It is noted that this case is subcritical. Agreement between the two results is seen to be quite good over the last 50% of the airfoil. Lack of agreement on the front portion of the surface is attributed to the alternative methods used to prescribe the airfoil slope by the respective codes. In particular, it is believed that the anomalous behavior near $\xi = 0.1$ in the LTRAN2 solution results from the cubic spline used to approximate the airfoil surface. Other than this behavior, the results compare reasonably well.

The unsteady lift coefficient as a function of time for a 1° pitching oscillation at a reduced frequency of 0.05 and freestream Mach number of 0.72 is displayed in Figure 2. Here the time origin is purely fictitious and has been introduced solely for the purpose of comparison. Respective time histories of lift calculated by each method were aligned at the maximum and minimum lift values for this, and subsequent figures. The results of the two methods are seen to compare exceptionally well except near the peak lift value. Even there, the predicted results are within 5% of each other. A comparison of the unsteady surface pressure coefficients corresponding

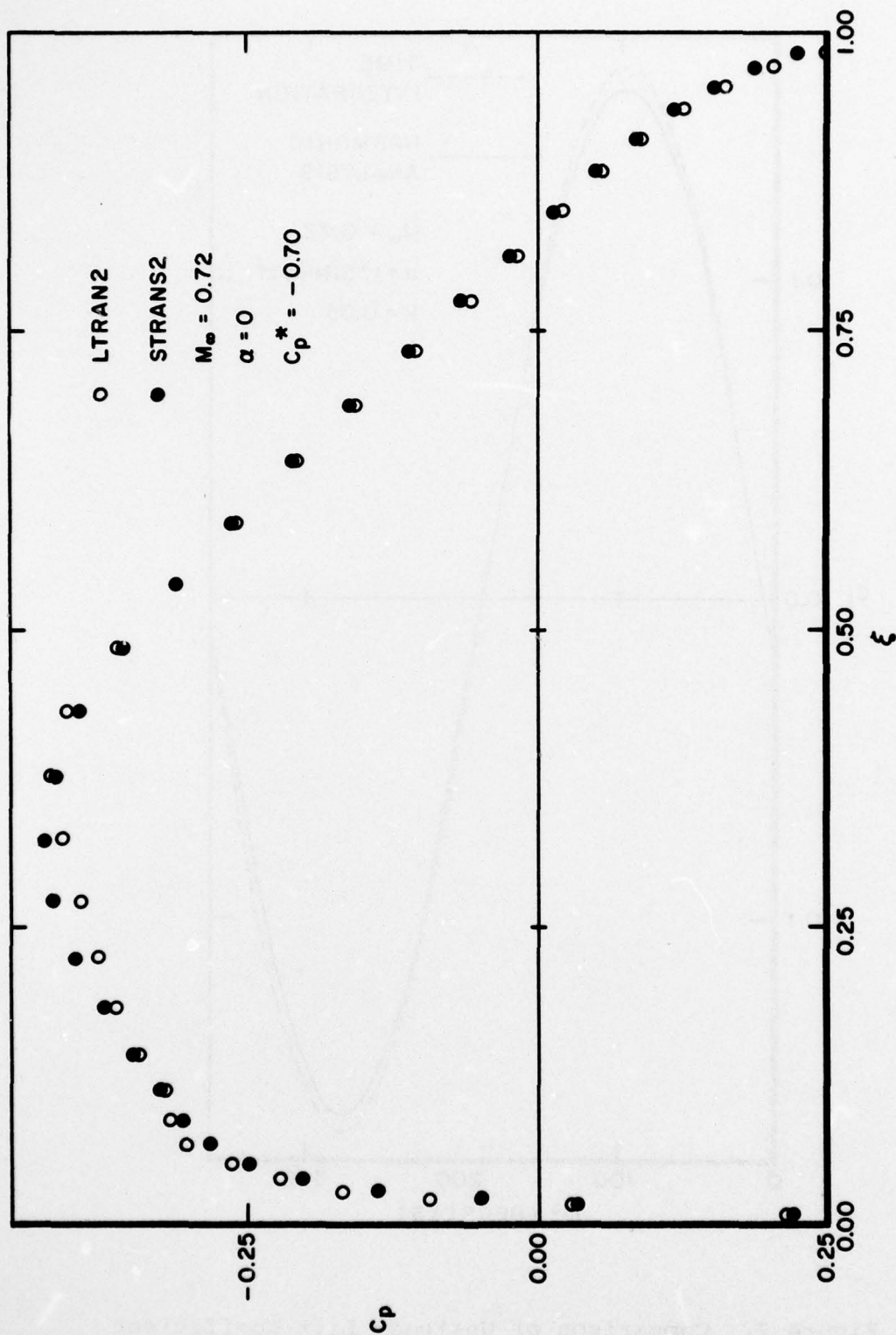


Figure 1. Comparison of Steady Surface Pressure for $M_\infty = 0.72$ and $\alpha = 0^\circ$.

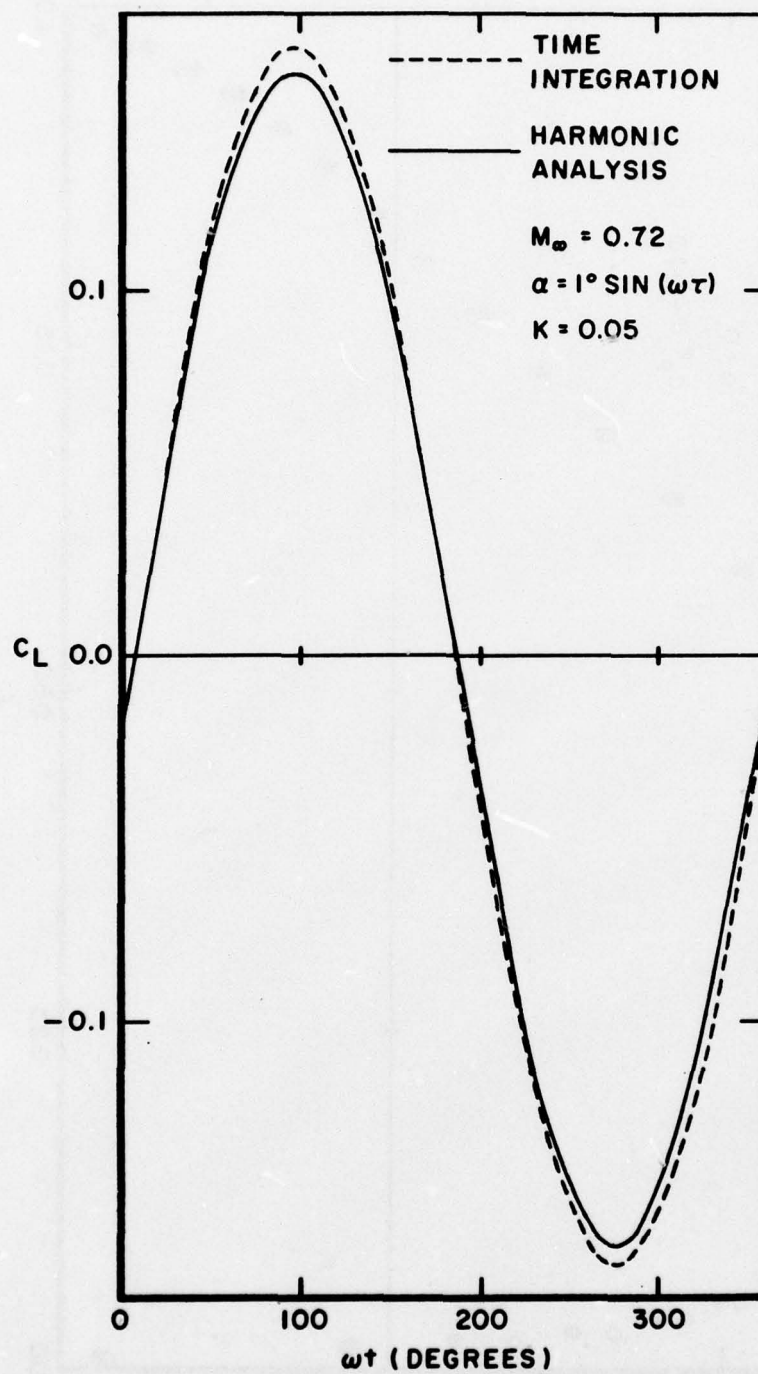


Figure 2. Comparison of Unsteady Lift Coefficient for a 1° Pitching Oscillation at $M_\infty = 0.72$ and $k = 0.05$.

to this case are shown in Figure 3. The time here was chosen as that at which the maximum lift occurred where the widest variation between the two results appeared. It is noted that the flow has remained subcritical. Generally the results compare quite favorably with the greatest discrepancy between the two methods again occurring over the front portion of the surface. The anomalous behavior in the initial profile (steady-state) of the time integration appears to have persisted into the unsteady result.

In Figure 4 the unsteady lift coefficient at the same Mach number and pitching displacement is displayed for a higher reduced frequency, $k = 0.20$. This comparison is quite similar to that seen at the lower frequency (Figure 2) with the maximum disagreement between the two results occurring at the peak lift value. It is interesting to note that both harmonic analysis and time integration indicate lower values for the lift coefficient at this higher frequency ($k = 0.20$) than were predicted for $k = 0.05$. In addition, for $k = 0.20$ time integration predicts a lower lift than harmonic analysis. The opposite behavior was observed for $k = 0.05$ (Figure 2). Corresponding unsteady surface pressure coefficients for this case are shown in Figure 5. Again these results are quite similar to those of the lower frequency case shown in Figure 3.

As a representative example of a comparison of supercritical calculations by the two computational methods, a freestream Mach number of 0.82 was selected. Steady-state surface pressure coefficients are shown in Figure 6. A well-defined shock is seen to lie

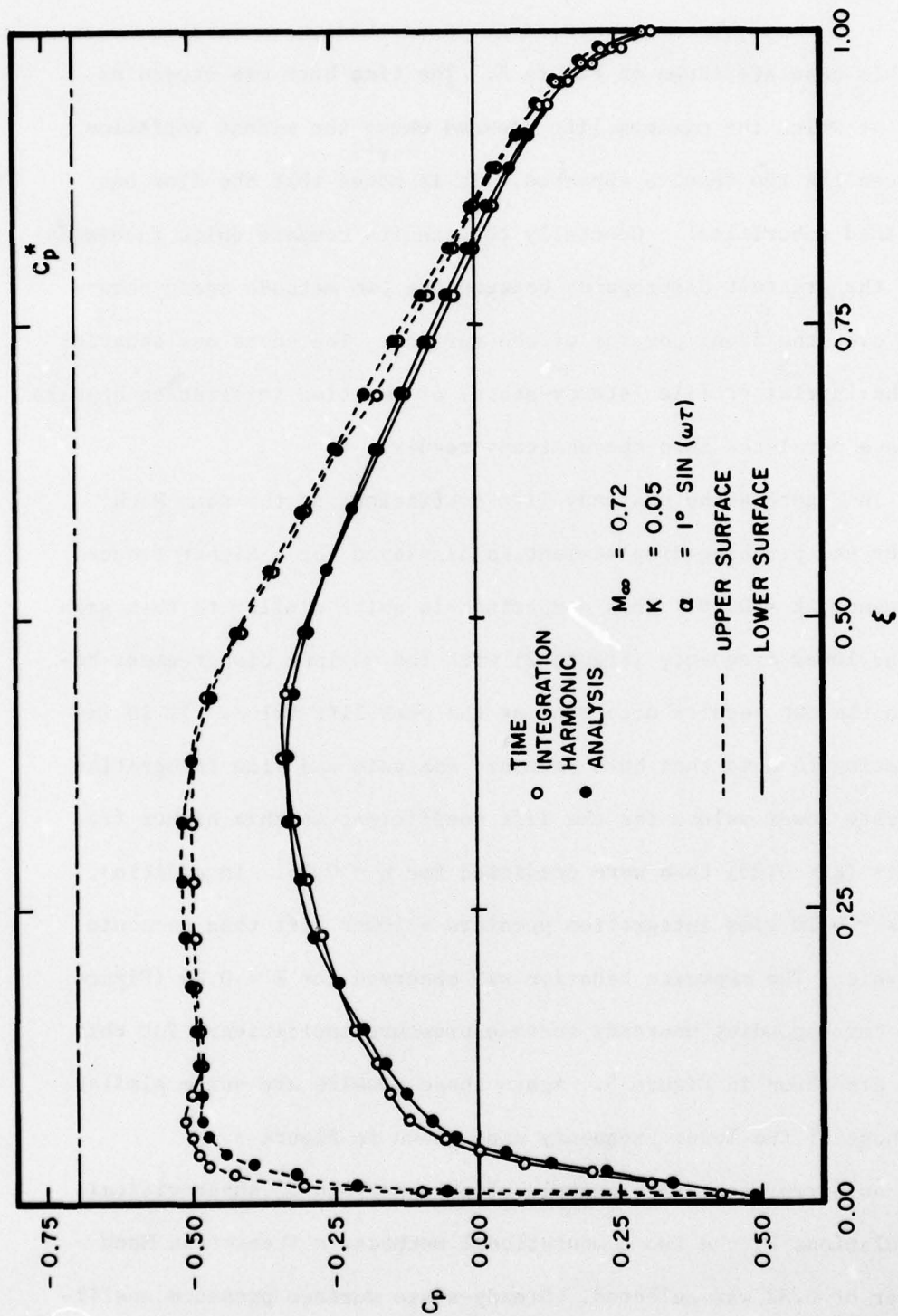


Figure 3. Comparison of Unsteady Surface Pressure Coefficient at Time Corresponding to Maximum Lift for a 1° Pitching Oscillation at $M_{\infty} = 0.72$ and $k = 0.05$.

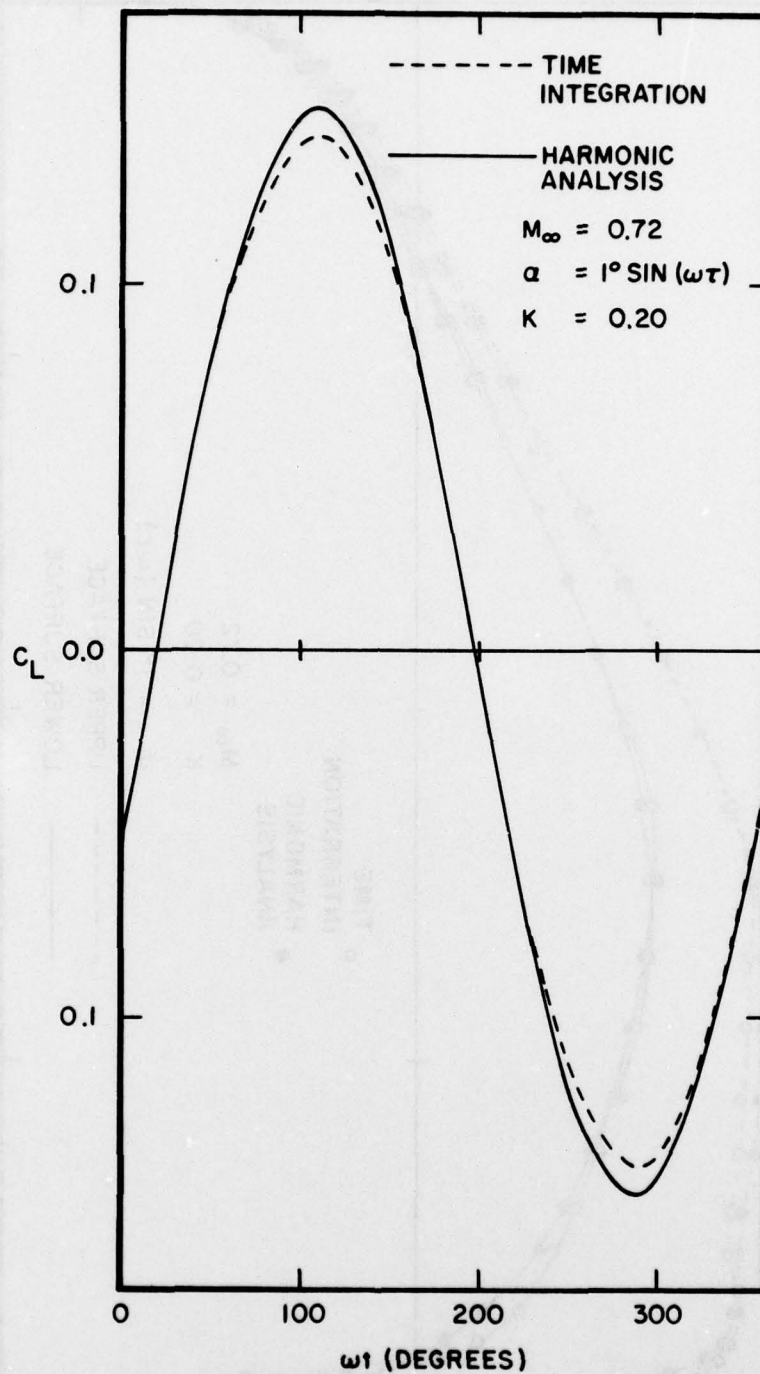


Figure 4. Comparison of Unsteady Lift Coefficient for a 1° Pitching Oscillation at $M_\infty = 0.72$ and $k = 0.20$.

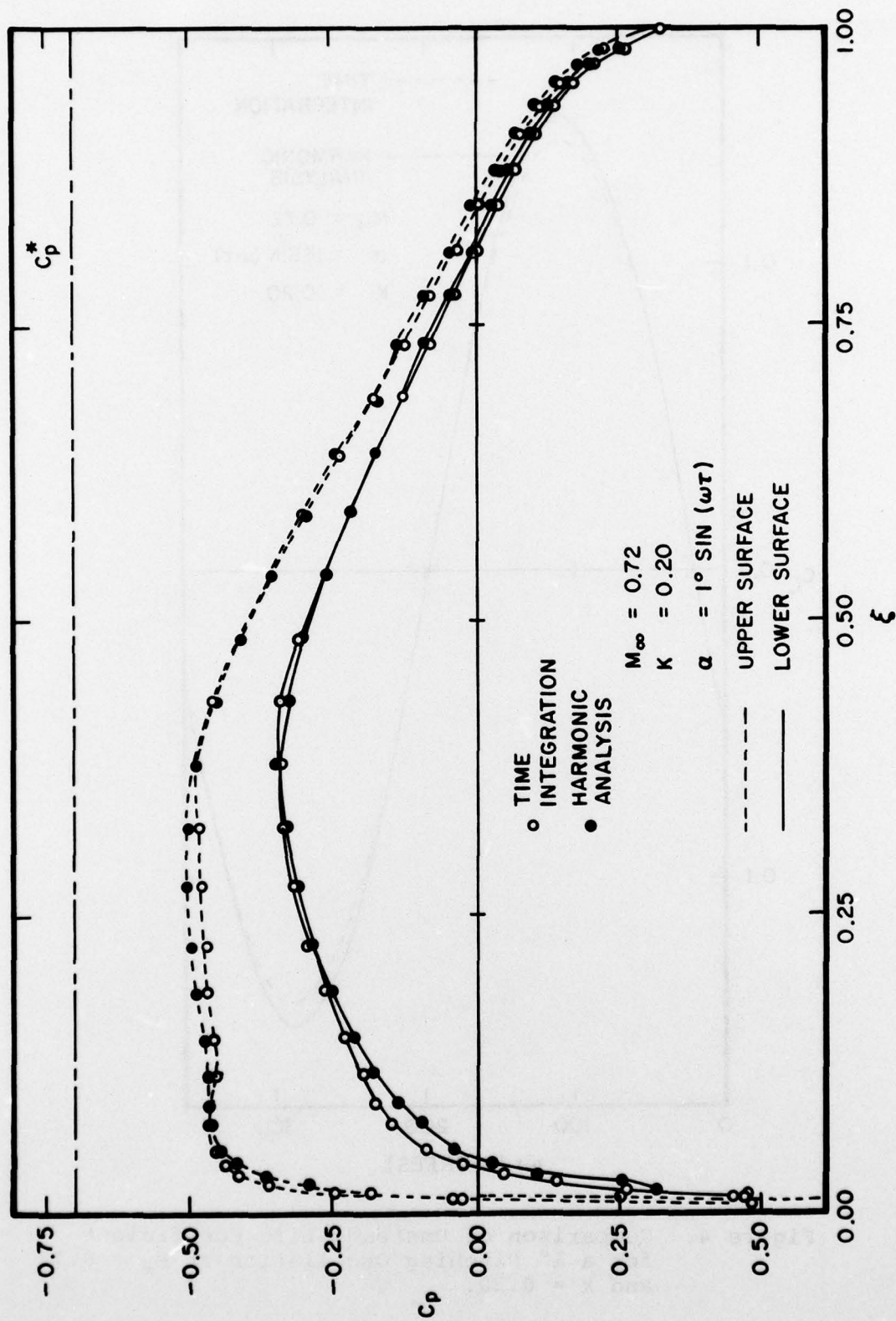


Figure 5. Comparison of Unsteady Surface Pressure Coefficient at Time Corresponding to Maximum Lift for a 1° Pitching Oscillation at $M_\infty = 0.72$ and $k = 0.20$.

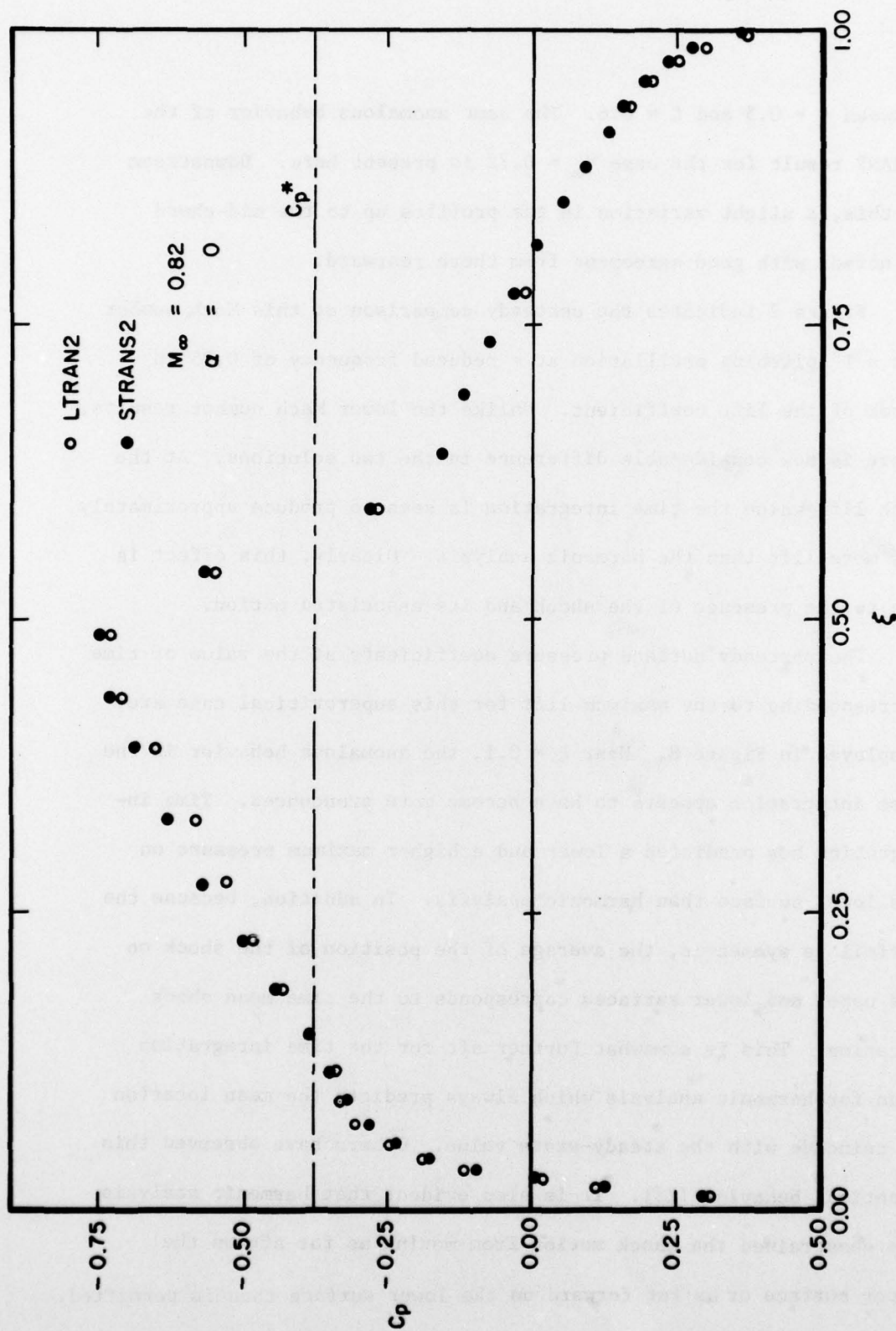


Figure 6. Comparison of Steady Surface Pressure Coefficient for $M_\infty = 0.82$ and $\alpha = 0^\circ$.

between $\xi = 0.5$ and $\xi = 0.6$. The same anomalous behavior of the LTRAN2 result for the case $M_\infty = 0.72$ is present here. Downstream of this, a slight variation in the profiles up to the mid-chord is noted, with good agreement from there rearward.

Figure 7 indicates the unsteady comparison at this Mach number for a 1° pitching oscillation at a reduced frequency of 0.05 in terms of the lift coefficient. Unlike the lower Mach number results, there is now considerable difference in the two solutions. At the peak lift value the time integration is seen to produce approximately 50% more lift than the harmonic analysis. Clearly, this effect is due to the presence of the shock and its associated motion.

The unsteady surface pressure coefficients at the value of time corresponding to the maximum lift for this supercritical case are displayed in Figure 8. Near $\xi = 0.1$, the anomalous behavior in the time integration appears to have become more pronounced. Time integration has predicted a lower and a higher maximum pressure on the lower surface than harmonic analysis. In addition, because the airfoil is symmetric, the average of the position of the shock on the upper and lower surfaces corresponds to the time mean shock location. This is somewhat further aft for the time integration than for harmonic analysis which always predicts the mean location to coincide with the steady-state value. Others have observed this identical behavior (23). It is also evident that harmonic analysis has constrained the shock motion from moving as far aft on the upper surface or as far forward on the lower surface than is permitted.

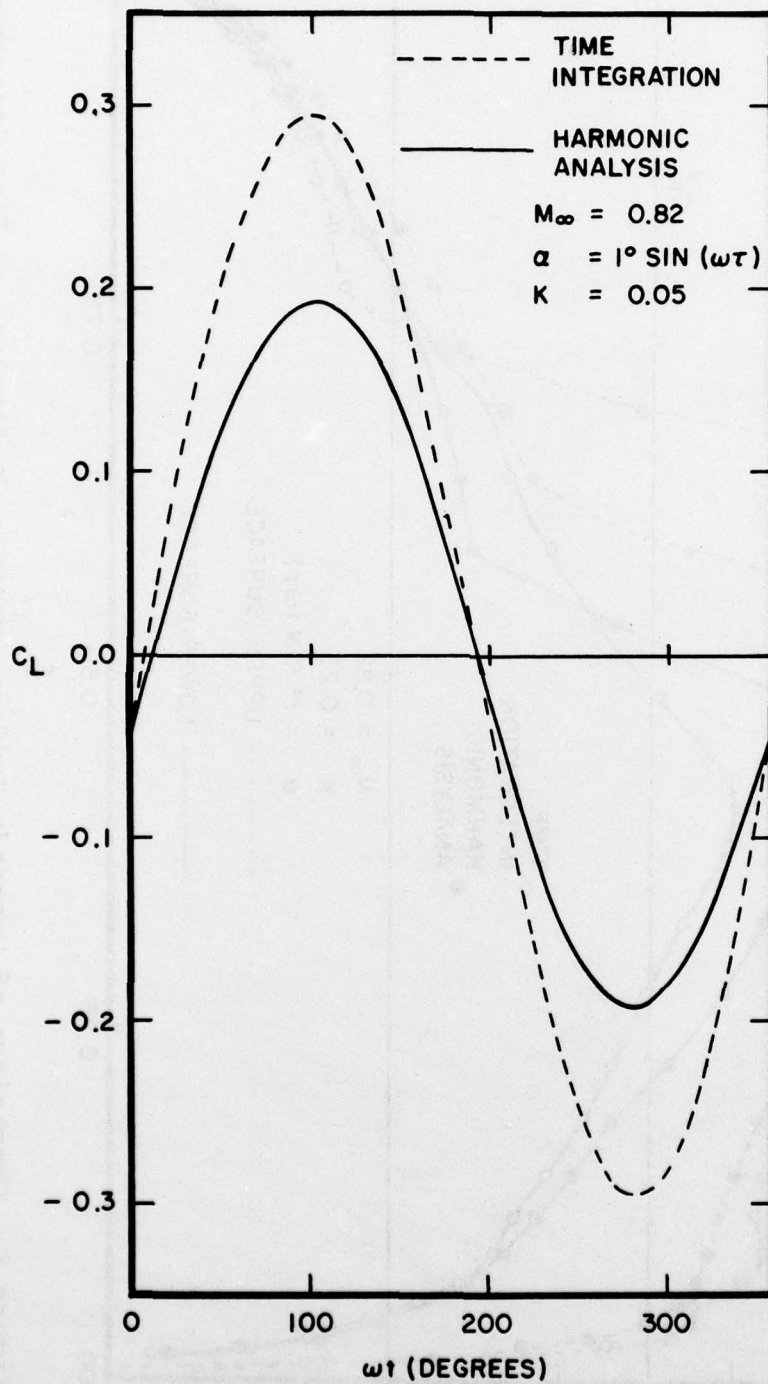


Figure 7. Comparison of Unsteady Lift Coefficient for a 1° Pitching Oscillation at $M_\infty = 0.82$ and $k = 0.05$.

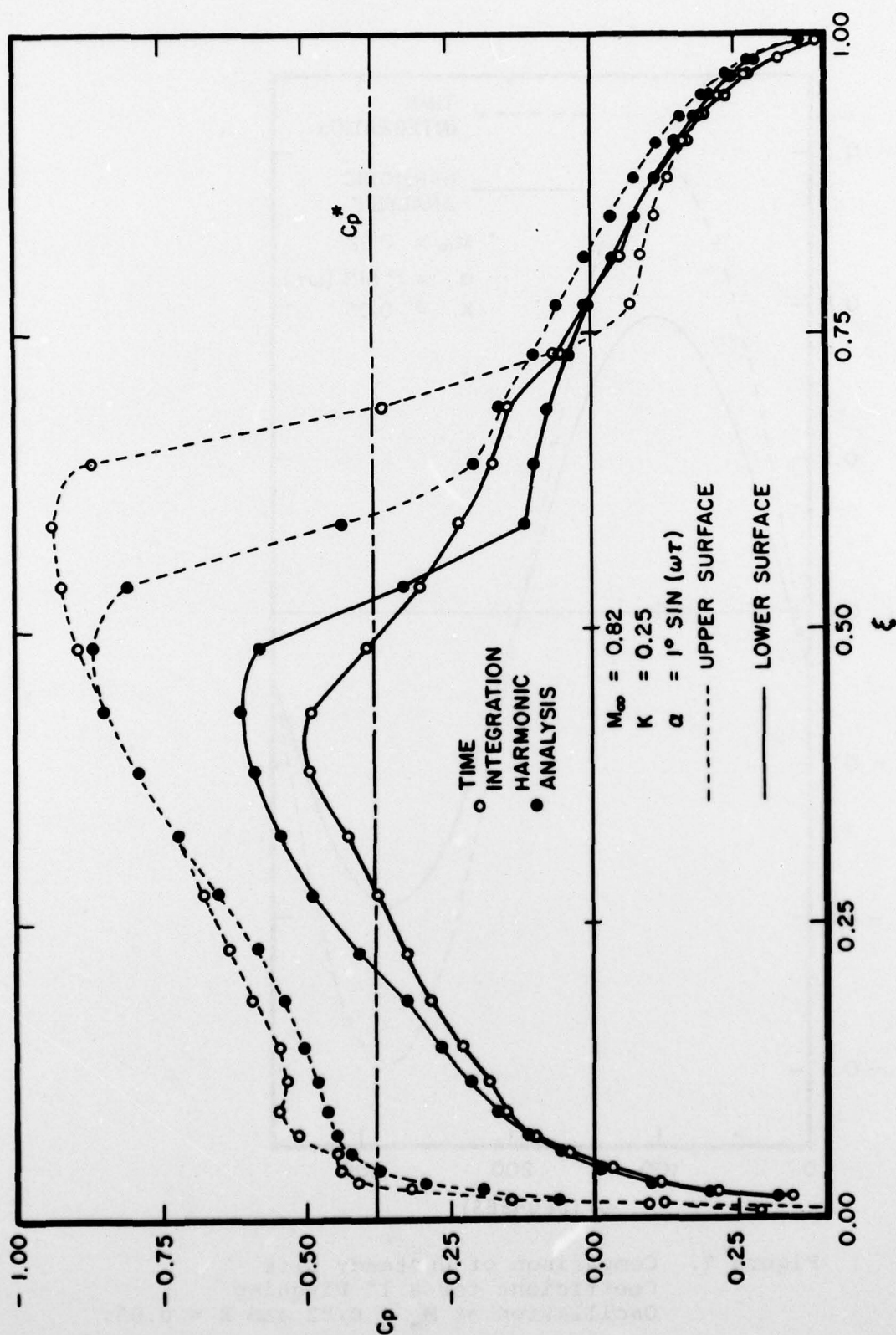


Figure 8. Comparison of Unsteady Surface Pressure Coefficient at Time Corresponding to Maximum Lift for a 1° Pitching Oscillation at $M_\infty = 0.82$ and $k = 0.05$.

by integrating in time.

In order to examine asymmetric behavior of the solutions generated by the two methods, the airfoil was oscillated about a non-zero angle of attack. Steady-state surface pressure coefficients at $M_\infty = 0.72$ and $\alpha = 1^\circ$ are displayed in Figure 9. This case is seen to be sub-critical and it is interesting to note that this steady result is quite similar to the two unsteady results at the same Mach number (Figures 3 and 5). The time varying lift coefficient for a 0.5° pitching oscillation about the steady 1° angle of attack for a reduced frequency, $k = 0.05$, is shown in Figure 10. Here the shape of the time history lift curve generated by each method is virtually identical. However, time integration predicts a higher time mean lift coefficient than that indicated by harmonic analysis. This corresponds to the same behavior as was observed for the case $M_\infty = 0.82$ where it was noted that harmonic analysis always recovers steady-state conditions as the time mean values, which is not necessarily true of time integration. Figure 11 indicates the comparison of surface pressures for this case at the time corresponding to maximum lift. The flow has remained just subcritical, with most of the discrepancy between the two results occurring near the leading edge. Abrupt changes in the slope of the pressure curve which are evident in time integrated profile may have resulted in loss of accuracy in the calculation of the lift coefficient through numerical integration.

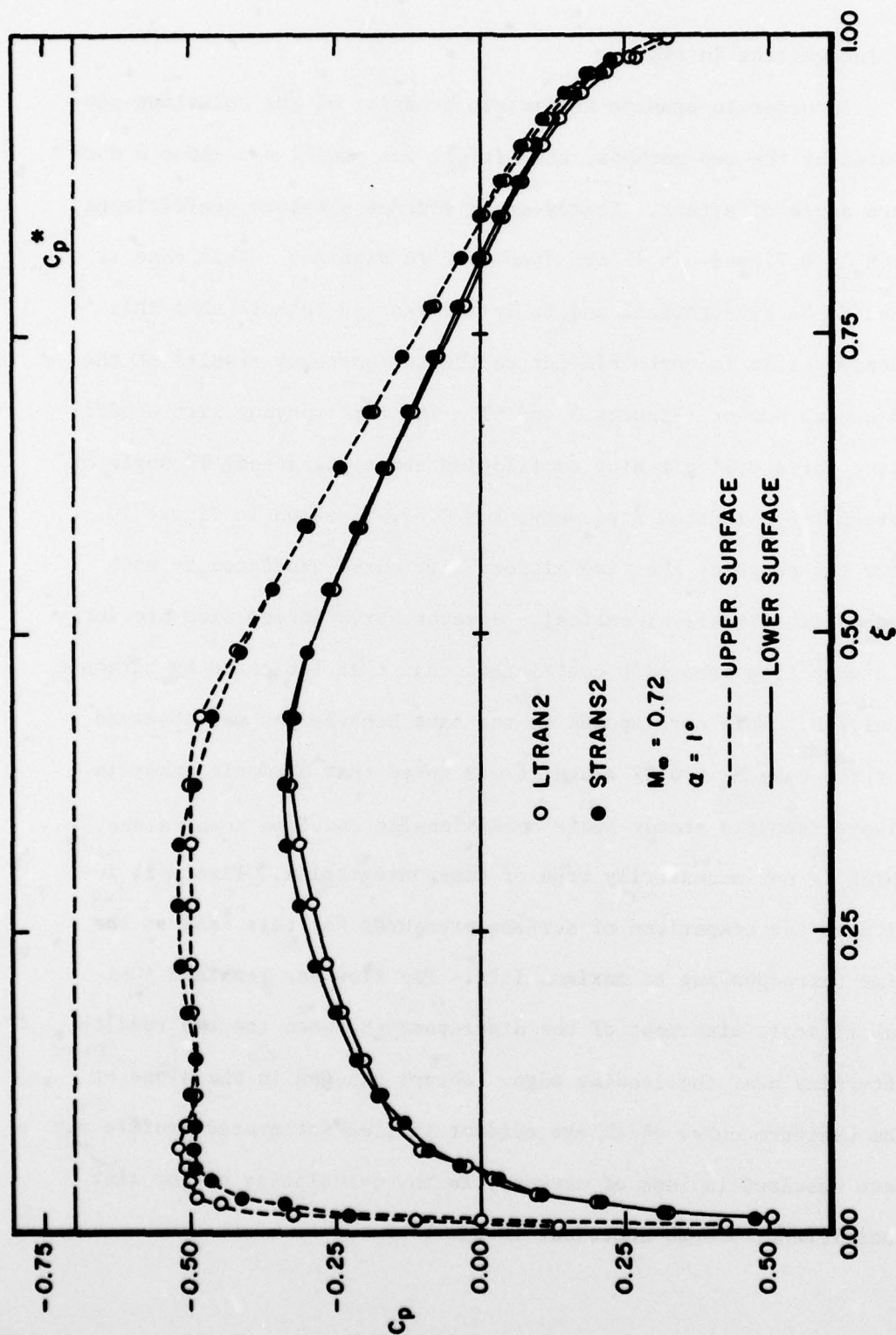


Figure 9. Comparison of Steady Surface Pressure Coefficient for $M_\infty = 0.72$ and $\alpha = 1^\circ$.

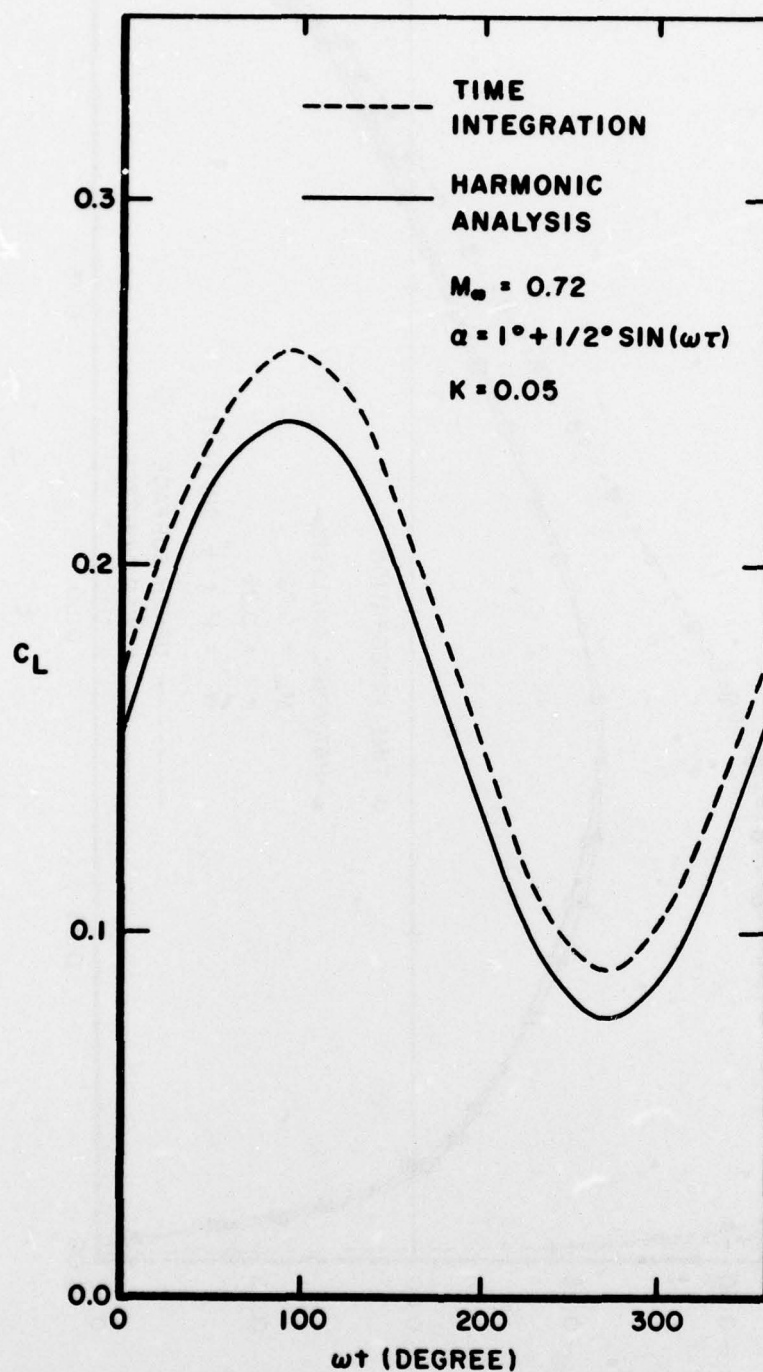


Figure 10. Comparison of Unsteady Lift Coefficient for a 0.5° Pitching Oscillation about a Mean Angle of Attack of 1° at $M_{\infty} = 0.72$ and $k = 0.05$.

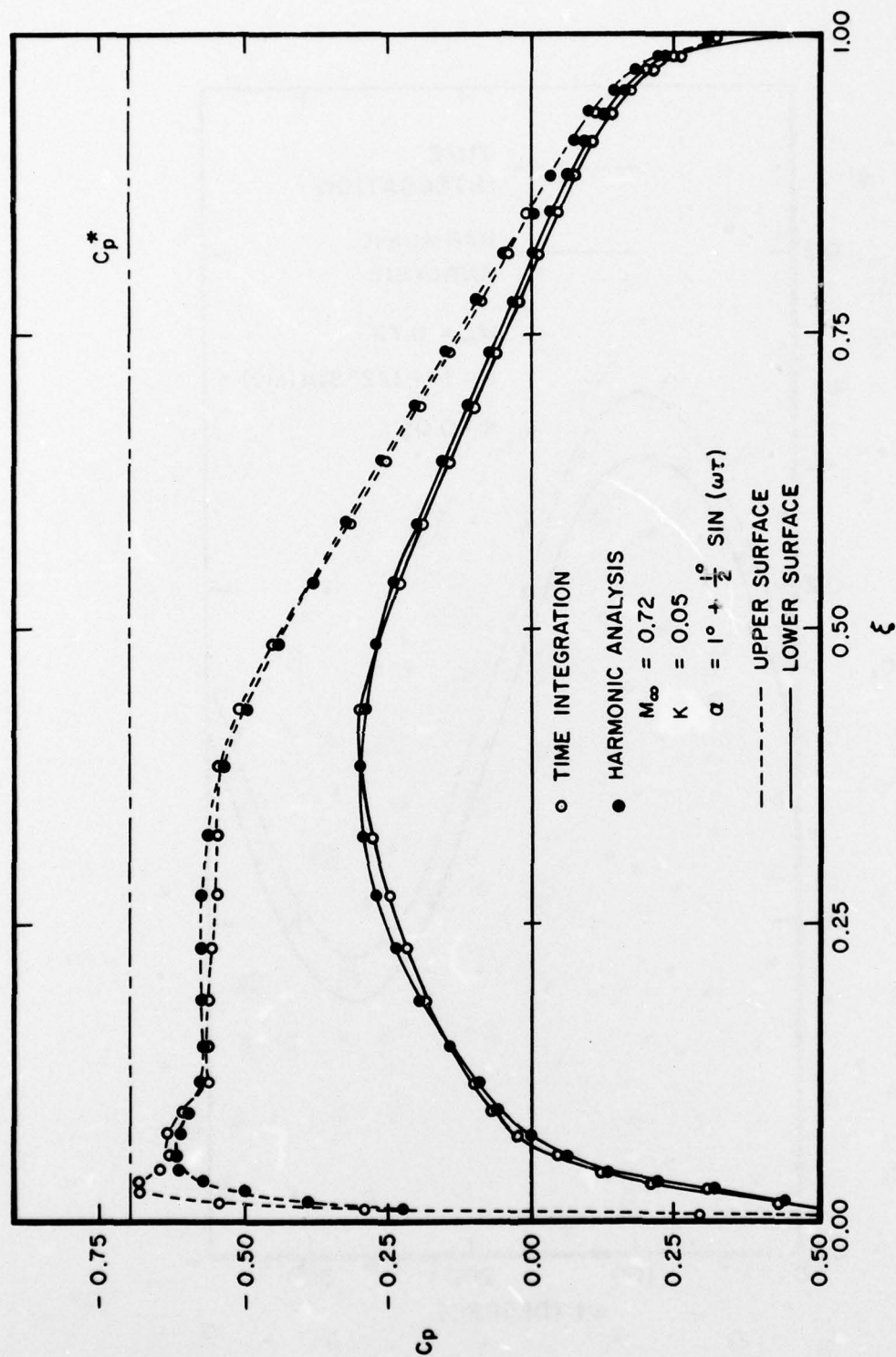


Figure 11. Comparison of Unsteady Surface Pressure Coefficient at Time Corresponding to Maximum Lift for a 0.5° Pitching Oscillation about a Mean Angle of Attack of 1° at $M_\infty = 0.72$ and $k = 0.05$.

SECTION VI

CONCLUSIONS

Solutions to the unsteady low frequency small disturbance transonic potential equation have been obtained by both the method of harmonic analysis and by the method of time integration for the pitching oscillation of an NACA 64A010 airfoil at several combinations of freestream Mach number, reduced frequency, and displacement amplitude. As far as was possible, computational differences in obtaining those solutions were minimized. When this could not be accomplished, these differences were noted. It is considered significant that all solutions were generated using an identical computational mesh in the immediate vicinity of the airfoil. The choice of free parameters corresponding to each particular case considered (M_∞ , k , pitching amplitude) was specifically restricted so as not to violate the inherent assumption of either method. The reduced frequency was never more than 0.20 as the low frequency approximation becomes a poor assumption above a value of about 0.40. Pitching amplitudes were specified to be 1° or less so as not to violate the small disturbance assumption. While harmonic analysis was not expected to predict large scale shock-wave motions with accuracy, a supercritical case was considered in order to deduce the range of acceptability for this method of analysis.

Comparisons between the solution methods were provided in terms of the time dependent lift coefficient and the unsteady surface

pressure coefficient. For oscillations in a subcritical flow field about a zero mean angle of attack the two methods were found to agree quite well. When a large shock appeared, harmonic analysis failed to reproduce the unsteady shock motion predicted by time integration. In the case of oscillation about a non-zero mean angle of attack, the unsteady lift obtained from the harmonic result varied by a simple translation from that resulting from integrating in time.

SECTION VII

REFERENCES

1. Ballhaus, W.F., Some Recent Progress in Transonic Flow Computations, VKI Lecture Series: Computational Fluid Dynamics, Rhode-St-Genese, Belgium, March 1976.
2. Ballhaus, W.F., and Goorjian, P.M., Computation of Unsteady Transonic Flows by the Indicial Method, AIAA Paper 77-447, March 1977.
3. Magnus, R.J. and Yoshihara, H., Inviscid Transonic Flow over Airfoils, AIAA Paper 70-47, January 1970.
4. Magnus, R.J. and Yoshihara, H., Calculations of Transonic Flow over an Oscillating Airfoil, AIAA Paper 75-98, January 1975.
5. Ballhaus, W.F., Magnus, R., and Yoshihara, H., Some Examples of Unsteady Transonic Flow, Proceedings of the Symposium on Unsteady Aerodynamics, Vol. II, pp. 769-791, 1975.
6. Magnus, R. and Yoshihara, H., The Transonic Oscillating Flap, AIAA Paper 76-327, July 1976.
7. Isogai, K., Calculation of Unsteady Transonic Flow over Oscillating Airfoils Using the Full Potential Equation, AIAA Dynamics Specialist Conference, San Diego, CA., March 1977.
8. Ehlers, F.E., A Finite Difference Method for the Solution of the Transonic Flow Around Harmonically Oscillating Wings, NASA CR-2257, 1974.
9. Traci, R.M., Albano, E.D., Farr, J.L., and Cheng, H.K., Small Disturbance Transonic Flows About Oscillating Airfoil, AFFDL-TR-74-37, June 1974.
10. Traci, R.M., Albano, E.D., and Farr, J.L., Small Disturbance Transonic Flows about Oscillating Airfoils and Planar Wings, AFFDL-TR-75-100, August 1975.
11. Weatherill, W.H., Sabastian, J.D., and Ehlers, F.E., On the Computation of the Transonic Perturbation Flow Fields Around Two- and Three-Dimensional Oscillating Wing, AIAA Paper 76-99, January 1976.

12. Traci, R.M., Albano, E.D., and Farr, J.L., "Perturbation Method for Transonic Flows About Oscillating Airfoil," AIAA Journal, Vol 14, No. 9, pp. 1258-1266, 1976.
13. Murman, E.M. and Cole, J.D., Calculation of Plane Steady Transonic Flows, AIAA Paper 70-188, June 1970.
14. Beam, R.M. and Warming, R.F., Numerical Calculations of Two-Dimensional, Unsteady Transonic Flows with Circulation, NASA TN D-7605, 1974.
15. Beam, R.M. and Ballhaus, W.F., Numerical Integration of the Small-Disturbance Potential and Euler Equations for Unsteady Transonic Flow, NASA SP-347, Part II, pp. 789-809, 1974.
16. Caradonna, F.X. and Isom, M.P., "Numerical Calculation of Unsteady Transonic Potential Flow over Helicopter Rotor Blades," AIAA Journal, Vol. 14, No. 4, pp. 82-488, 1976.
17. Ballhaus, W.F. and Goorjian, P.M., Implicit Finite Difference Computations of Unsteady Transonic Flows about Airfoils, Including the Treatment of Irregular Shock-Wave Motions, AIAA Paper 77-205, January 1977.
18. Beam, R.M., and Warming, R.F., "An Implicit Finite Difference Algorithm for Hyperbolic Systems in Conservation-Law Form," Journal of Computational Physics, Vol. 22, No. 1, pp. 87-110, 1976.
19. Ballhaus, W.F. and Steger, J.L., Implicit Approximate-Factorization Schemes for the Low-Frequency Transonic Equation, NASA TM X-73, 082, 1975.
20. Farr, J.L., Traci, R.M., and Albano, E.D., Computer Programs for Calculating Small Disturbance Transonic Flows About Oscillating Airfoils, AFFDL-TR-74-135, November 1974.
21. Olsen, J.J. and Andries, R.A., Surface Fitting to Cambered Airfoils, AFFDL-TM-76-78-FBR, August 1976.
22. Klunker, E.B., Contribution to Methods for Calculating the Flow About Thin Lifting Wings at Transonic Speeds, NASA TN D-6530, 1971.
23. Hafez, M.M., Rizk, M.H., Murman, E.M., and Wellford, L.C., Numerical Studies of the Unsteady Transonic Small Disturbance Equation, Flow Research Report No. 85, August 1977.